Low biodegradability of particulate organic carbon mobilized from thaw slumps on the Peel Plateau, NT, and possible chemosynthesis and sorption effects

Sarah Shakil[1], Suzanne E. Tank[1], Jorien E. Vonk[2], Scott Zolkos[1,3]

5   [1]Department of Biological Sciences, University of Alberta, Edmonton, Canada
[2]Department of Earth Sciences, Vrije Universiteit, Amsterdam, The Netherlands
[3]current address: John A. Paulson School of Engineering and Applied Sciences, Harvard University, Cambridge, MA, 02138, USA

10   *Correspondence to*: Sarah Shakil (shakil@ualberta.ca)

Abstract. Upon thaw, permafrost carbon entering streams may be mineralized into CO_2 or re-sequestered into sediments. The balance between these processes is an important uncertainty in the permafrost-carbon-climate feedback. Warming and wetting in the western Canadian Arctic are accelerating thaw-driven mass wasting by permafrost thaw slumps, increasing particulate organic carbon (POC) delivered to headwater streams by orders of magnitude. Using aerobic incubations of POC from streams

15 affected by thaw slumps we find that slump-mobilized POC undergoes minimal (~ 4%) oxidation over a 1-month period and may be predominantly destined for sediment deposition. Mobilization of mineral-rich tills in this region may also protect carbon from mineralization via adsorption to minerals and promote inorganic carbon sequestration via chemolithoautotrophic processes. Region-specific assessments of permafrost carbon fates and inquiries beyond organic carbon decomposition are needed to constrain drivers of carbon cycling and climate feedbacks within stream networks affected by permafrost thaw.

1 Introduction

Permafrost soils comprise the single largest pool of terrestrial organic carbon (OC) (Schuur et al., 2015; Hugelius et al., 2014), half of which may be vulnerable to rapid mobilization into modern biogeochemical cycles via abrupt thaw processes (Turetsky et al., 2020; Olefeldt et al., 2016). Permafrost dissolved organic carbon (DOC), typically defined as compounds < 0.7µm, is highly susceptible to biotic mineralization into CO_2 within aquatic systems (Vonk et al., 2015a; Littlefair and Tank, 2018;

25 Abbott et al., 2014; Mann et al., 2015). Abrupt thaw can mobilize orders of magnitude more particulate organic carbon (POC, typically > 0.7µm) than DOC, yet the biodegradability of permafrost POC is not well understood (Shakil et al., 2020; Tank et al., 2020; Vonk et al., 2015b). Suspended particles can be important sites for mineralization (Attermeyer et al., 2018) or mineral protection (Hemingway et al., 2019; Opfergelt, 2020; Groeneveld et al., 2020). In addition to molecular composition and a host of environmental factors that typically affect organic matter decomposition (e.g., microbial activity, nutrient availability)

30 (Kothawala et al., 2021), mineralization of POC in stream networks depends on transport vs. deposition within those networks. When settled out, mineralization of POC can be reduced by ~50% (Richardson et al., 2013) or more, particularly if contained in anoxic sediments (Peter et al., 2016). Fractions of POC with different density and size therefore not only experience a different settling and transport trajectory, but also may have differing processes and rates affecting OC dynamics (Tesi et al., 2016). If biodegradability varies across size and density fractions, this could alter realized mineralization during transport

35 relative to measurements on bulk OC (Tesi et al., 2016).

Warming and intensifying precipitation across the ice-rich terrain of the Peel Plateau in western Canada has triggered an acceleration of thaw-driven landscape erosion in the form of retrogressive thaw slumps (hereafter, slumps) (Kokelj et al., 2020). Slump-DOC in the region has an elevated lability compared to reference streams without slumps, as shown by chemical composition and incubations (Littlefair et al., 2017; Littlefair and Tank, 2018). Slump-POC chemical composition suggests

40 lower bioavailability (Shakil et al., 2020; Bröder et al., 2021), though POC bioavailability has not been experimentally assessed. Given that slump-released carbon occurs almost entirely as POC in this region (Shakil et al., 2020), understanding the fate of this carbon remains a critical knowledge gap.

Our objectives were to assess the potential for slump POC to be mineralized to CO_2 during transport in streams. To do this, we undertook experimental incubations to: (a) determine whether slump-POC differs in biodegradability from POC present in
45 unimpacted waters; and (b) quantify and assess the biodegradability of slump-POC fractions relative to their transport potential. This work provides insight into the fate of an understudied component of permafrost-mobilized OC.

2 Methods

2.1 Region and field sampling

Slumping across the Peel Plateau (Fig. 1) typically mobilizes terrestrial material from three distinct sources: (1) Pleistocene-
50 age tills that have remained preserved within permafrost since deposition by the Laurentide Ice Sheet and subsequent permafrost aggradation; (2) Holocene-age permafrost developed from tills following active layer deepening and/or slumping in previous warm periods; and (3) a contemporary active layer. Thus, relative contribution of sources to streams can depend on thaw depth (Shakil et al., 2020; Bröder et al., 2021). Variation in source composition can also vary west-east as vegetation (elevation) and geology changes along this gradient (Shakil et al., 2020).

55 Sampling occurred during July-August, within the Stony Creek and Vittrekwa River watersheds of the Gwich'in Settlement Region on the Peel Plateau (Fig. 1). In 2015, substrate from streams near and within three slump sites was used to test if mobilization of slump-POC and nutrient release affect biodegradability of OC in streams (Shakil et al., 2020). Stream water samples were obtained from: channelized runoff within each thaw slump (IN); a downstream location where all runoff entered the valley-bottom stream (DN); and an unimpacted reference stream upstream of slump inflow (UP) (Fig. 1b). Site HD-UP
60 experienced some encroachment of slump runoff, and thus was not a fully unimpacted site (Fig. S5). In 2016, substrate was collected upstream, within, immediately downstream, and 2.79 km downstream of slump SE to assess variations in biodegradability with transport potential. In 2019, substrate was collected within and downstream of slump FM3 to follow-up results from 2015 and 2016 (details below). Slump sites had varied elevation and morphology, with maximum headwall heights (Fig. 1a) ranging from 7.1 to 23m (Shakil et al., 2020). For further sample collection details, see supplementary S1.
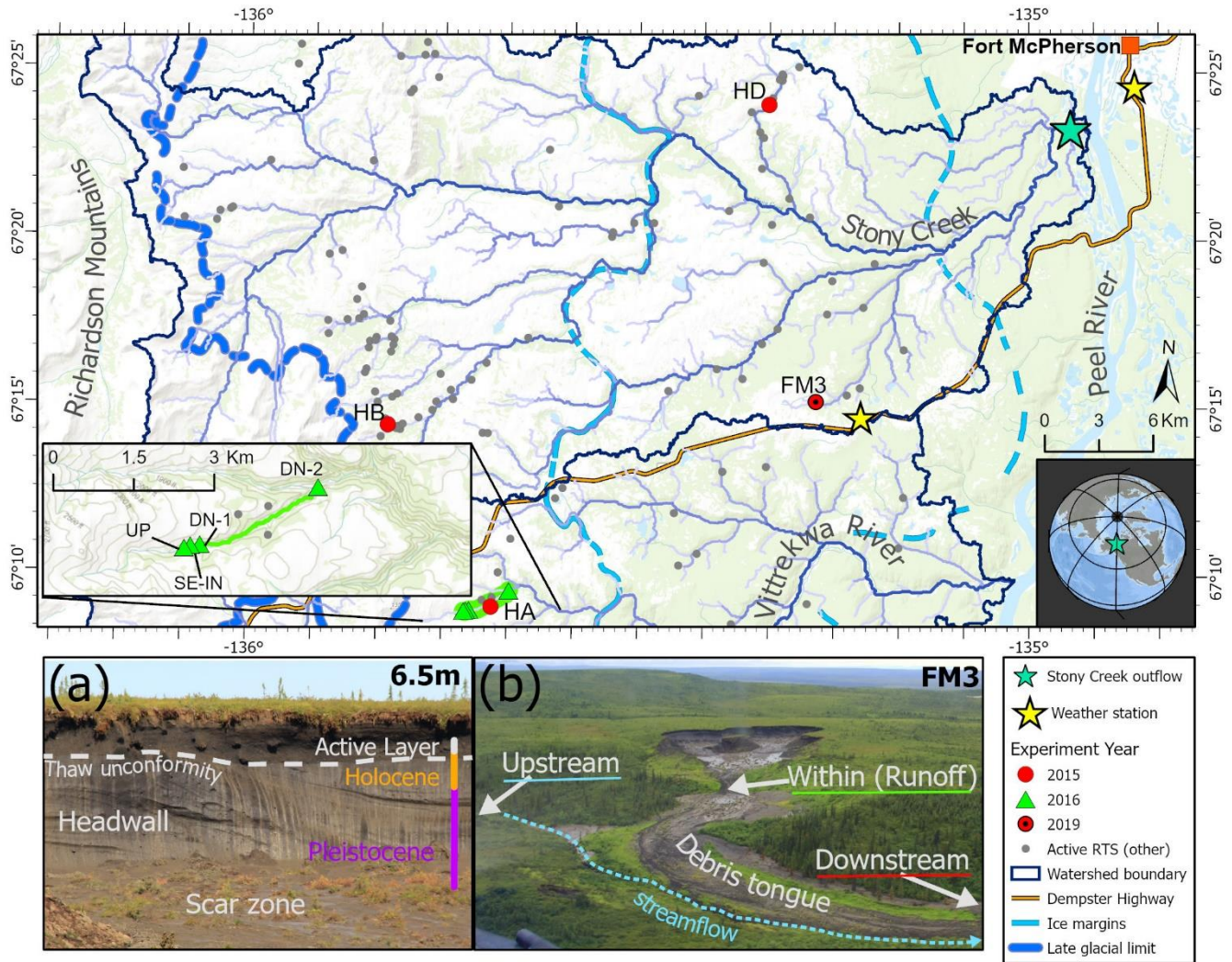
65
Figure 1: Location of slump sites sampled for experiments. 2016 sampling points (green triangles) show sampling locations along a transect which began just upstream of the point where slump SE runoff enters a valley bottom stream. Watershed boundary in inset is of the Peel River Watershed with the Stony Creek outflow marked for reference. Panel (a) shows headwall units of a slump. Panel (b) shows stream sampling points relative to a slump site. Active RTS features are from Segal et al. (2016). Former glacial limits of the Laurentide Ice Sheet (ice margins and late-glacial limit) are delineated from Duk-Rodkin and Hughes (1992). Service Layer credits: (1) World Topographic Map: Northwest Territories, ESRI, © OpenStreetMap contributors, HERE, Garmin, USGS, NGA, EPA, USDA, NPS, AAFC, NRCan. (2) World Ocean Base: Esri, Garmin, GEBCO, NOAA NGDC, and other contributors. (3) World Continents.

2.2 Biodegradation experiments

2.2.1 2015 Experiment: Effects of POC source, dissolved constituents, and settling

To test the effect of POC source (Table 1), we incubated unfiltered upstream water (upstream POC; treatment "UU") and filtered upstream water with a 2 mL addition of slump runoff (slump POC; "SU") in 120 mL glass serum bottles for 7 days at
80 ca. 20°C in the dark, with continuous end-over-end rotation (4 rpm) (supplementary S2, Fig. S5). Control bottles accounted for DOC contained in filtered upstream water alone (no POC control; "UF"). Additionally, we tested for: (a) the effect of particle deposition by allowing a replicate set of SU bottles to settle out ("SS"); and (b) the slump-derived release of additional solutes (e.g., nutrients) by mixing slump POC with filtered downstream water ("SD").

2.2.2 2016 Experiment: Variability as a function of transport potential

85 SE within-slump runoff was split into three sieve size fractions (63 – 2000 µm, 20 – 63 µm, < 20 µm) by sieving a 0.5 mL aliquot and adding the resultant size fractions to filtered downstream water in 60 mL glass BOD bottles (supplementary S2, Fig. S6). An unfractionated control (0.5 mL in 60 mL downstream water) was also created, and bottles were incubated for 8 days in the dark at ca. 20°C as above. Since relative concentrations of each size fraction were maintained, the <20 µm fraction had orders of magnitude greater total suspended solid (TSS) concentrations than the larger two (Table S2). We also incubated
90 filtered and unfiltered (but diluted, Table S2) stream water from upstream, downstream, and 2.79 km downstream of SE to accompany size fraction incubations. We characterized OC differences between size fractions using: (a) 14C age, (b) percent OC (i.e., OC: TSS), and (c) absorbance and fluorescence spectra of based-extracted particulate organic matter (BEPOM) (Osburn et al., 2012)(supplementary S3).

2.2.3 Measurements

95 We measured: (a) concentrations of DOC, POC, and TOC, and $SUVA_{254}$ (an optical proxy for dissolved organic matter (DOM) aromaticity) (Weishaar et al., 2003) at the beginning and end of incubations; and (b) O_2 concentrations ~daily (PreSens, Fibox4, SP-PSt3-NAU-D5-YOP) to provide insight on rate of change (Richardson et al. 2013). We assumed heterotrophic breakdown of OC would be the dominant O_2 consumption pathway, as respiratory quotients across several freshwater sites have been noted to vary around 1 (Berggren et al., 2012). Incubation O_2 concentrations presented never dropped below 2 mg L^{-1}; a
100 threshold well above O_2 limiting concentrations for different bacterial species (Stolper et al., 2010 and references therein). One exception was one of four replicates for the SE unfractionated treatment, which was removed and replaced with the mean of replicates for statistics. Our experiments aimed to mimic conditions downstream, thus slump-affected incubations had POC concentrations ranging from 1.4 to 18.6 times DOC concentrations. Samples for TSS concentration were collected alongside POC. Further details in supplementary S3.

105 **2.2.4 Follow-up experiments**

First, to assess processes that may have contributed to O_2 loss coupled with OC gains observed in 2015 and 2016, we undertook two follow up experiments. First, we combined 0.15 mg of sterilized HD debris tongue sediments (collected in 2016)(Zolkos and Tank, 2020) with 18.2 Ω Milli-Q (MQ) water to assess abiotic O_2 loss. We incubated 60 mL glass BOD bottles on a shaker table in the dark at ca. 20°C for 7 days, monitoring O_2 as above. Second, we measured change in dissolved and particulate

110 inorganic carbon (DIC, PIC), in addition to change in DOC and POC, in an incubation combining FM3 slump runoff with downstream water, including sterilized replicates. The treatments were designed to replicate treatment "SD" in 2015. Sterilization was achieved by autoclaving and adding $ZnCl_2$ as a poison and was validated using plate counts (supplementary S4). We hypothesized chemosynthesis associated with nitrification and sulfide oxidation (eqns. 2-4) could generate OC and so we additionally measured dissolved inorganic nitrogen (NH_4^+, NO_3^-, NO_2^-) and sulfate (SO_4^{2-}). Sediments in sterilized and

115 unsterilized bottles were characterized using X-ray diffraction (XRD) (supplementary S3.4).

$$NH_3 + 1.5O_2 \leftrightarrow NO_2^- + H^+ + H_2O \qquad\qquad (1a)$$
$$NO_2^- + 0.5O_2 \leftrightarrow NO_3^- \qquad\qquad (1b)$$

120 $$CO_2 + H_2S + O_2 + H_2O \leftrightarrow [CH_2O] + H_2SO_4 \qquad\qquad (2)$$

$$FeS_2 + 3.75O_2 + 3.5H_2O \leftrightarrow + 2H_2SO_4 + Fe(OH)_3 \qquad\qquad (3)$$
$$H_2SO_4 + 2(Ca,Mg)CO_3 \leftrightarrow 2(Ca^{2+}, Mg^{2+}) + SO_4^{2-} + 2HCO_3^- \qquad\qquad (4)$$
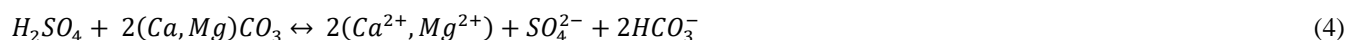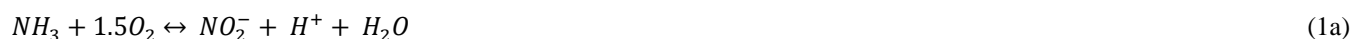
125 Note that equation 2 is a general equation of chemolithoautotrophic reduced sulfur oxidation that can have a variable stoichiometry and assumes sulfur oxidizing bacteria exclusively produce SO_4^{2-}, rather than both SO_4^{2-} and S^0 ((Klatt and Polerecky, 2015; Nelson et al., 1986). Equation 3 shows a net reaction for a model of pyrite oxidation at circumneutral-pH (Percak-Dennett et al., 2017). This sulfide oxidation can generate sulfuric acid that can weather carbonates (e.g., eq. 4) or silicates (Zolkos and Tank, 2020; Zolkos et al., 2020).

130 **2.3 Data analyses**

Two-way ANOVAs, with site and treatment as fixed effects, were used to assess the effect of POC presence (UF vs SU), source (UU vs SU), dissolved matrix (SU vs SD), and settling (SU vs SS) on percent changes in OC (DOC, POC, and TOC), DOM aromaticity (SUVA$_{254}$) and O_2 loss rate. One-way ANOVAs were also used to assess differences in the aforementioned changes between size fractions (2016 experiment). Two-way ANOVAs were used to assess the effect of distance and filtration

135 (fixed effects) for the 2016 transect experiments. Significant interactions/main effects were followed up with Tukey-adjusted pair-wise t-tests (Zar, 2010). We also calculated 95% confidence intervals to evaluate whether OC changes significantly

differed from zero. Principal components analyses were used to visualize differences in optical indices between size fractions (2016), and changes in DOM and BEPOM (2019). To assess factors controlling in situ CO2 and O2 dynamics we calculated departures of O_2 and CO_2 from atmospheric equilibrium (Vachon et al. 2019) using 2015 in situ measurements of dissolved

140   O_2 at several slump sites (Shakil et al., 2020) and coupled CO_2 departures (Zolkos et al., 2019). For further details, see Appendix A. Data for this publication is available through Shakil et al. (2021).

3 Results

3.1 Experiment 2015: Effects of POC presence and source

Across experiments, declines in POC were not observed, and in some cases, POC increased (Fig. 2). Slump runoff addition

145   into filtered upstream water (SU) did not significantly alter %ΔDOC, ΔSUVA254 (change in DOM aromaticity), or %ΔTOC ($p>0.05$; Table A1, Fig. 2) relative to the upstream filtered control (UF). Similarly, POC source (slump [SU] vs. unfiltered upstream [UU]) did not significantly affect %ΔTOC or ΔSUVA254 ($p>0.05$, Table A1, Fig. 2). However, %ΔPOC were significantly lower when particles were sourced from slump runoff (UU vs. SU; $p<0.001$, Table A1), potentially because particle concentrations were orders of magnitude lower in upstream bottles (Table S2). DOC increased in the presence of

150   upstream particles (UU) but decreased in the presence of slump particles (SU), though this difference was marginally insignificant (Table A1, $p = 0.053$). Despite no effect on %ΔTOC (Table A1), the addition of slump particles (SU) did significantly increase rates of O_2 consumption compared to upstream filtered and unfiltered treatments (UF and UU; Fig. 2 A-C), though this effect was dependent on slump site (significant interactions, Table A1; note lack of increase for site HD where slump runoff encroached upstream site).

155

Table 1. Summary of experiments and main results with reference to figures and text sections for details.

Year	Field Sampling	Exp. Details	#days	Test	Treatments	Main result	Considerations
2015	UP, IN, and DN of slumps HA, HB, HD	Sec. 2.2.1, Fig. S5	7	POC presence	**SU** *(slump in filtered upstream)* vs. **UF** *(filtered upstream)*	(1) between treatments: no effect on %ΔTOC but increased O_2 loss; (2) within treatments: no sig. TOC loss *(Fig 2, Table A1)*	
				POC source	**SU** vs. **UU** *(unfiltered upstream)*		
				Dissolved constituents	**SU** vs. **SD** *(slump in filtered downstream)*	(1) Between treatments: no effect on %ΔTOC or O_2 loss; (2) within treatments: no sig. TOC loss *(Fig 2, Table A1)*	
				Settling	**SU** vs. **SS** *(SS off rotator to allow settling)*	(1) Between treatments: no effect on %ΔTOC, reduced O_2 loss; (2) within treatments: no sig. TOC loss *(Fig 2, Table A1)*	
2016	UP, IN, DN, and 2.79 km DN of slump SE	Sec. 2.2.2, Fig. S6	8	Biodegradability vs. transport potential	Sieve size fractions: (1) 2000-63µm (2) 63-20µm (3) <20µm). + unfractionated reference	No sig. diff. in %Δ TOC or %Δ POC changes between size fractions but sig. TOC gain and largest DOC loss for particles <20 µm *(Fig 2, Table A2)*	↓ [TSS] in two larger size fractions relative to smallest, two largest also within MQ error
				Transect validation	unfiltered and filtered DN vs. 2.79km DN. + UP reference	Change in downstream distance: no effect on %ΔTOC; within treatments: no sig. TOC loss *(Fig 2, Table A3)*	UP and 2.79 km DN within MQ blank error
2018	HD debris tongue material	Sec. 2.2.4	7	Abiotic O_2 loss	Sterilized debris tongue sediments in Milli-Q (MQ) water vs. MQ control	Rapid O_2 loss in absence of microbial activity *(Fig S3a)*	MQ may accelerate weathering, HD debris sediments an extreme weathering endmember
2019	IN and DN of slump SC	Sec. 2.2.4, Fig. S7	27	paired inorganic carbon changes & chemo-lithotrophy	Unsterilized mimic of **SD** (2015 treatment) vs. sterilized **SD.** + MQ blanks	Prior gains not replicated but only ~4% of TOC mineralized, greater sulfate gains and nitrification in unsterilized treatments *(Fig 4)*	SC slump in a different landscape type than SE and HA where prior gains were observed, sterilization treatments may not be a true abiotic control
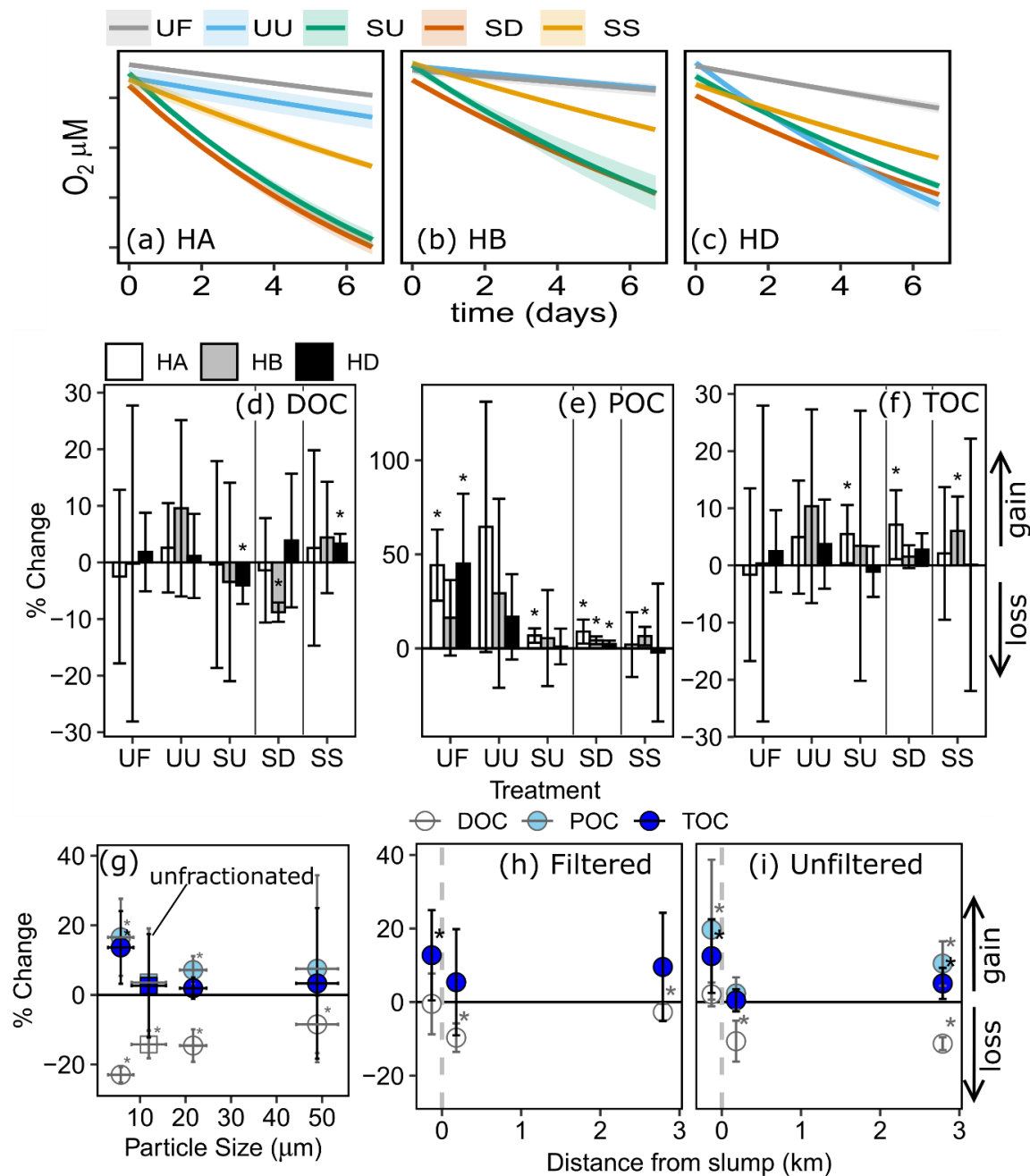
Figure 2: (a-c) Measured (point) and modelled (line) O₂ (mg L⁻¹) across combinations of source material and settling effects. Percent change in DOC, POC, and TOC in comparison to: **(d-f)** combinations of source material and settling effects; **(g)** geometric mean particle size; and **(h-i)** distance from slump site. Vertical errors are 95% confidence intervals with asterisks marking significant differences from zero. Horizontal errors **(e)** are particle size geometric standard deviation. Codes **(a-f)**: filtered (UF) and unfiltered (UU) upstream, slump material in upstream (SU) and downstream (SD) filtrate, and SU settled out (SS). HA, HB, and HD are slump sites.

3.2 Experiment 2015: Effects of background dissolved constituents and settling

Changing filtrate to downstream water, which has higher ion and nutrient concentrations (Shakil et al. 2020), had no significant effect on any parameter measured in the experiment (SU vs. SD, Table A1). Allowing slump particles to settle (SU vs SS) did not affect %ΔTOC but did significantly reduce O_2 consumption rates. Mean DOC concentrations also switched from decreasing to increasing (Fig. 2D, though the difference was not significant; p=0.10, Table A1).

3.3 Experiment 2016: Variability dependent on transport potential

Based on 14C age, %POC, and relative contribution of fluorescent peak C (Coble, 2007), larger particle size fractions appeared to be associated with fresher terrestrial-origin organic matter than smaller size fractions (Appendix B). POC associated with particles < 20 µm dated to > 27,000 cal BP, while POC associated with particles ranging from 20 – 63 µm and 63 – 2,000 µm dated to ~ 19,600 cal BP and ~8,000 cal BP respectively (Table B1).

Only bottles containing particles <20 µm displayed significant gains in TOC (95% CI; Fig. 2G-I) but we did not find a significant difference in %ΔTOC or %ΔPOC between size fractions (ANOVA; Table A2). DOC losses occurred in all treatments downstream of slumps, to a greater degree when particles were present (i.e., unfiltered treatments) (Fig. 2H-I, p<0.05 Table A3), and were significantly greater when particles were <20 µm (p<0.05, Fig. 2G, Table A2). Increases in SUVA254 were also significantly greater for <20µm particle treatments (p<0.05 Table A2 and C1), as were TSS concentrations (Table S2). %DOC loss was also significantly greater 2.79 km downstream of SE compared to immediately downstream (Table A3).

3.4 O₂ vs. carbon

Change in O_2 and TOC generally did not follow the 1:1 trend expected if heterotrophic respiration dominated metabolic processing (Fig. 3 A-C). The greatest deviations from 1:1 was observed in treatments containing slump runoff, where despite large losses in O_2, we saw non-significant changes to gains in TOC. Increases in TOC from upstream, filtered, and 2.79 km downstream bottles were within the range of experimental blanks (Figure 3C).

The rate of O_2 consumption within and across experiments was generally greater in treatments with greater initial TSS (Fig. 3D). However, there was no consistent relationship between TOC changes and initial TSS (Fig. 3E), but some of the greatest TOC increases occurred during incubations of SE particles <20 µm and HA slump particles in upstream (SU) and downstream (SD) filtrate, treatments amongst those with the greatest initial TSS (Fig. 3A, B, E).

In-situ comparisons of O_2 vs. CO_2 showed within-slump samples to have the greatest excess CO_2, with several samples substantially departing from the 1 CO_2: -1 O_2 stoichiometry associated with heterotrophic respiration (Fig. 3F). In contrast, several downstream and upstream sites display measurements close to atmospheric equilibrium for CO_2 but are supersaturated for O_2, potentially due to temperature changes and lower solubility of O_2 (Vachon et al., 2020).
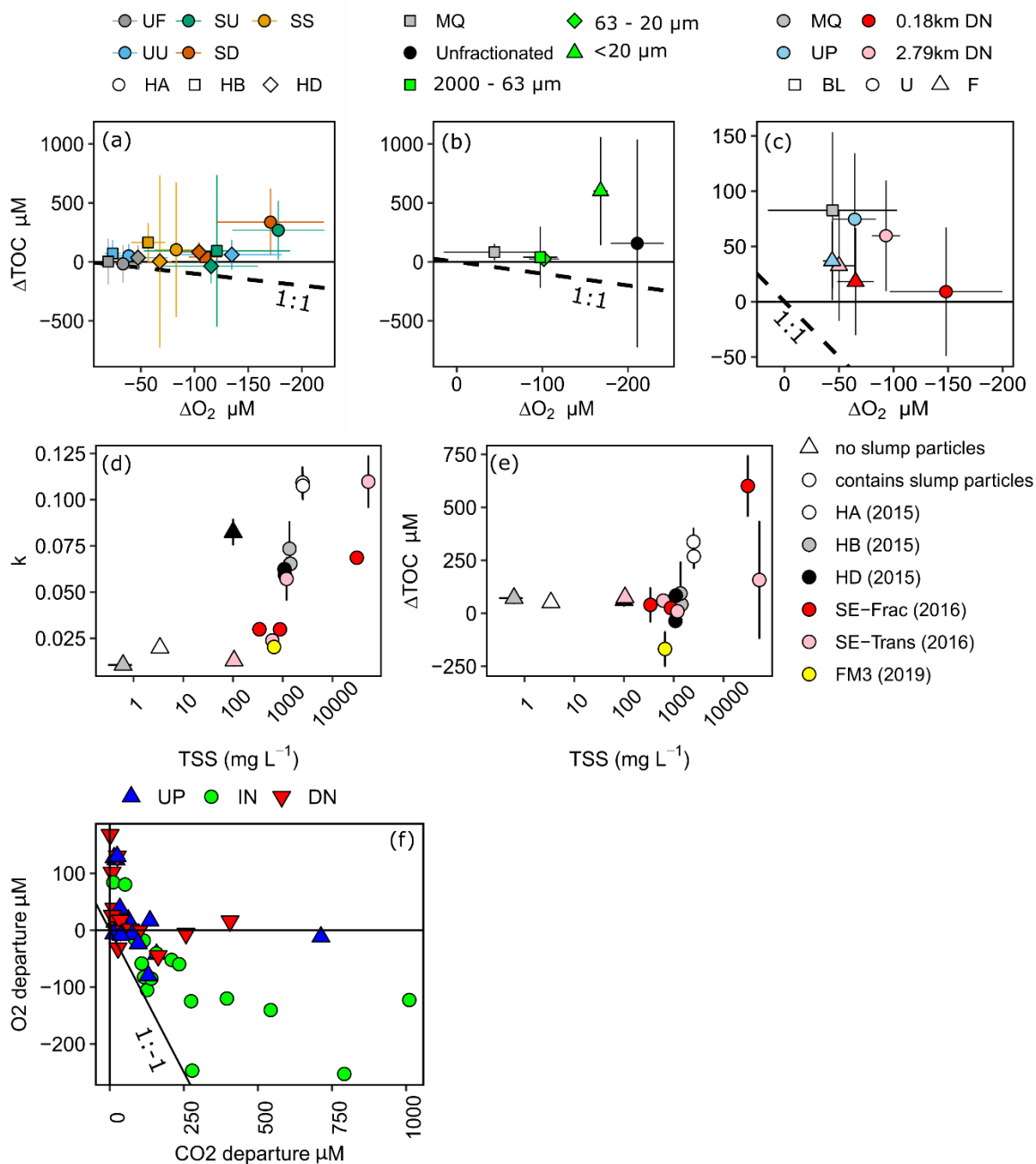
Figure 3: Changes in TOC vs. changes in dissolved O_2 for: (a) test of biodegradability; (b) site SE fractionation experiment; and (c) site SE transect experiment. Dashed lines in a-c represent predicted loss of OC for respiratory quotient=1 and error bars show 95%
200 **confidence intervals. (d-e) Exponential rate of O_2 consumption (k) or changes in TOC vs. initial TSS for treatments across experiments, excluding filtered, settled, and sterilized treatments from a-c. SE-Frac indicates the fractionated treatments from panel (b). (f) Departures of O_2 and CO_2 from atmospheric equilibrium in samples collected upstream (UP), downstream (DN) and within (IN) a series of slump sites on the Peel Plateau. Error bars in (d) and (e) show standard error of the mean. Codes in (a): filtered (UF) and unfiltered (UU) upstream, slump material in upstream (SU) and downstream (SD) filtrate, and SU settled out (SS). HA, HB,**
205 **and HD are slump sites.**

3.5 Follow-up experiments

3.5.1 2018 test: sterilized debris sediments in Milli-Q water

Oxygen was completely consumed (~226 µM) in bottles containing sterilized HD debris tongue material suspended in Milli-
210 Q water within 4-5 days, exceeding the O_2 loss rates previously observed (Table S1, Fig. S3a). Bottles containing sterilized
sediments had lower pH (5.52 – 6.09) following incubation than MQ controls (6.53 – 6.91).

3.5.2 2019 test: inorganic carbon changes and potential chemolithotrophy

Oxygen consumption occurred in sterilized treatments (-15 ± 6 µM, mean ± 95% CI, t = 27 days) but was more pronounced
in unsterilized bottles (-124 ± 15 µM). The pronounced O_2 decline in unsterilized bottles was accompanied by a significant
215 loss of DOC (-83 ± 26 µM) and a non-significant loss of POC (-85 ± 261 µM), balancing to a non-significant loss of TOC (-
170 ± 262 µM, Fig. 4). Total inorganic carbon (TIC) increased significantly in unsterilized treatments, driven by increases in
DIC. In sterilized bottles, modest oxygen losses were accompanied by significant DOC losses (-93 ± 51 µM), significant POC
gains (141 ± 33 µM), balancing to a modest non-significant gain in TOC (48 ± 66 µM). TIC had a minor significant decrease
(-25 ± 20 µM), driven by losses in DIC.
220 Ammonium decreased from 8.68 ± 0.47 µM to below detection (0.2 µM) in unsterilized bottles, while nitrite and nitrate
increased by 2.58 ± 2.36 and 1.33 ± 1.67 µM, respectively. In sterilized bottles, ammonia increased by 6.74 ± 1.80 µM
alongside negligible changes in nitrate or nitrite. Sulfate generation was greater in unsterilized (90 ± 6 µM) than sterilized (54
± 23 µM) bottles, but for both treatments sulfate increased more than would be expected via pyrite oxidation (Fig. 4D, based
on oxygen stoichiometry in eq. S3). However, the only sulfur-bearing mineral detected in sediments (XRD; 1-5% detection
225 limit, this study) was pyrite.
A biplot of PCA components 1 and 2 did not reveal any shifts in BEPOM or DOM optical characteristics during incubation of
unsterilized treatments (Fig. 4D-E). However, DOM from sterilized treatments shifted towards lower molecular weight (SR,
slope ratio), lower aromatic material (SUVA$_{254}$) of greater biological origin (BIX). PC1 separated DOM in sterilized and
unsterilized bottles, suggesting sterilization processes increased the proportion of simple compounds which cautions against
230 assuming the sterilized treatment is a true abiotic control of organic matter changes.
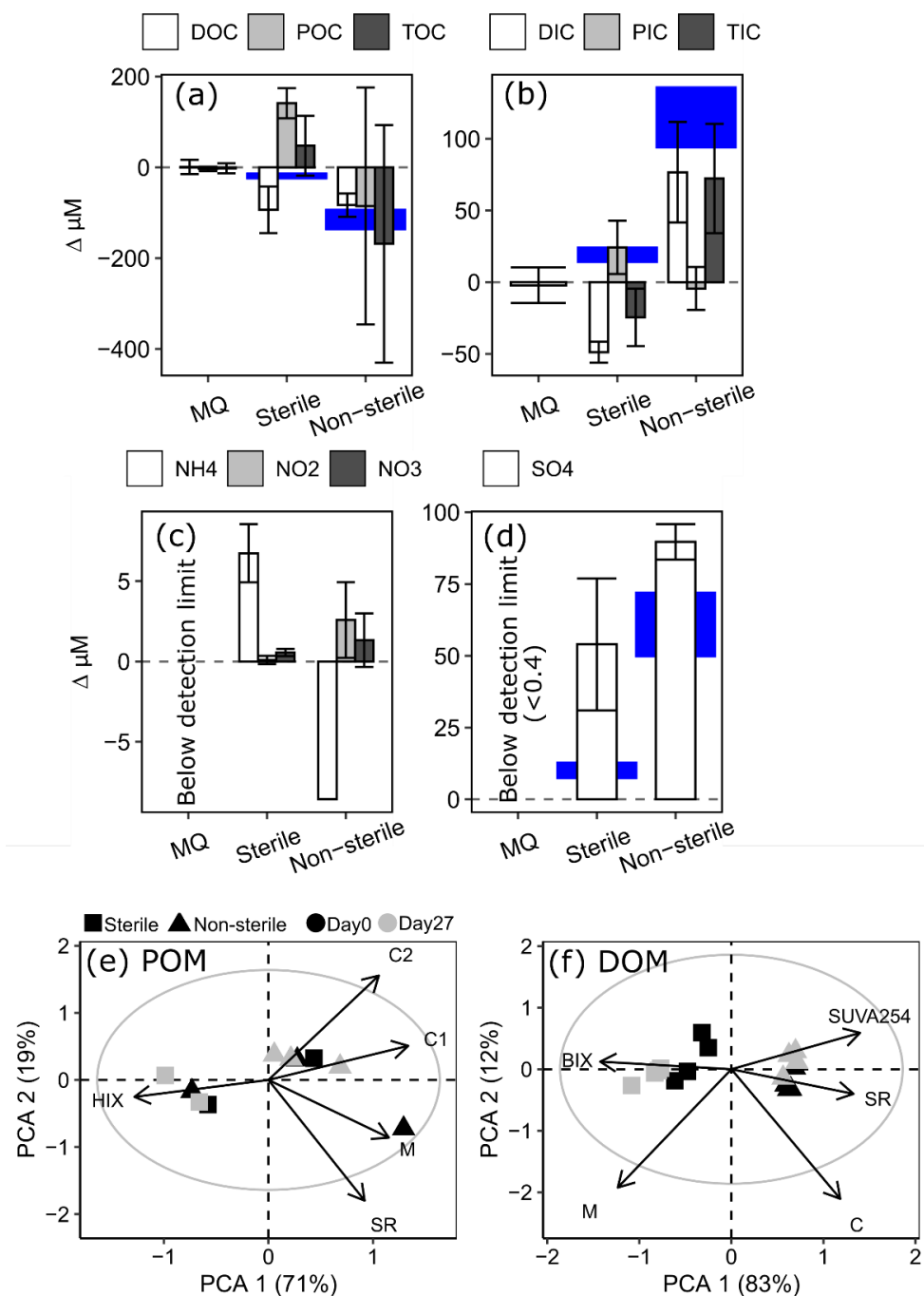
Figure 4: Changes in millimolar concentrations of: (a) organic carbon; (b) inorganic carbon; (c) ammonium (NH$_4^+$), nitrite (NO$_2^-$), and nitrate (NO$_3^-$); and (d) sulfate (SO$_4^{2-}$) in 2019 test of interferences. Note difference in scales between panels. Blue shades highlight

235 **potential carbon gains or losses based on O$_2$ loss and a respiratory quotient of 1 (a-b) and potential sulfate generated from pyrite oxidation (eq. 3). Error bars and blue heights both show a range representing 95% confidence intervals. (e-f) PCA biplot of components 1 and 2 showing variation in POM (e) and DOM (f) optics. Grey circle outlines circle of equilibrium contribution, plot shown in scaling 1.**

4 Discussion

Our incubations, coupled with multiple studies examining slump-POC composition (Shakil et al., 2020; Bröder et al., 2021; Keskitalo et al., 2021) indicate that slump-mobilized POC in glacial landscapes of western Canada has low biodegradability on the Peel Plateau. We found no significant losses of POC or TOC or evidence that %ΔTOC increased in streams due to slump-mobilized POC across slump sites and for varying size fractions and distances downstream of slump SE. While %ΔTOC did not significantly differ across size fractions of slump SE particles, particles most likely to remain in transport (< 20 µm) enabled the greatest loss in %ΔDOC (linked to greater TSS) and significant gains in TOC. A coupled transect experiment showed that downstream of SE, TOC gains were not significant or were within error of blanks (2.79 km downstream), though both downstream treatments had orders of magnitude lower TSS than the <20 µm size fraction treatment sourced directly from slump runoff.

The lack of biodegradability contrasted elevated O_2 consumption rates downstream of slumps, except for slump HD, where slump runoff encroached into the upstream site (Fig. S4). OC gains suggest potential for chemoautotrophic carbon sequestration. Further, abiotic processes (e.g., mineral oxidation) appear to have the potential to consume oxygen rapidly enough to decouple oxygen and carbon dynamics from the 1:1 relationship associated with heterotrophic respiration, as suggested by sterile incubations of HD debris material. The excess in situ CO_2 concentrations we observe are likely from mineral weathering that can generate CO_2 in this system (Zolkos et al., 2018).

Our finding of low POC biodegradability is likely conservative since incubations focus on the most labile period (7-27 days) (Richardson et al., 2013). Our longest incubation (27 d; Fig. 4 non-sterile) did not show significant TOC losses, though 95% error spanning losses expected from a 1:1 relationship with O_2 suggests that detection of change may be masked by error in POC measurements (Fig. 4a). Using ΔTIC as an alternate metric of carbon mineralization, we estimate that ~ 4% of the initial TOC pool may have been mineralized within 27 d. Time series experiments on TOC degradation from similarly glacially-conditioned Qikiqtaruk (Herschel Island) indicate that CO_2 production ceased by the end of a 120-day incubation, and greater than half (~58%) of total CO_2 was produced within the first 27 d. Assuming a similar pattern for OC mineralization, we estimate ~7% of slump-mobilized TOC on the Peel Plateau may be readily mineralized during transport in streams. These findings are consistent with measures of little change in CO_2 concentrations downstream relative to upstream of slumps (Zolkos et al., 2019), despite orders of magnitude increases in POC and TOC (Shakil et al., 2020). We note that rapid within-slump processing of labile components prior to entrainment within streams may still occur, as supported by high NH_4^+ concentrations (Shakil et al., 2020) indicative of decomposition (Tanski et al., 2017), low representation of labile compounds in the slump scar zone and stream sediments relative to headwall sources (active layer)(Keskitalo et al., 2021), and excess CO_2 in slump runoff resulting from both heterotrophic respiration and geogenic production (Zolkos et al., 2019)(Fig. 3F). OC rapidly lost

270 within-slump likely predominantly originates from the active layer (Bröder et al., 2021) and Holocene-age permafrost in areas where organic material buried in colluvial deposits from past slumping has preserved organics (Lacelle et al., 2019).

In addition to serving as a possible marker for decomposition, high concentrations of ammonia may stimulate nitrification and associated chemosynthetic carbon sequestration. Though we did not see significant TOC gains in our 2019 experiment, ammonia loss coupled with nitrite production suggests active nitrification. Nitrifying bacteria have slow growth rates (Sinha

275 and Annachhatre, 2007; Bock and Wagner, 2013), with the molar ratio of NH_4^+ consumed to carbon fixed ranging from 25 – 100 (Ward 2013). Using this stoichiometry and initial ammonia concentrations estimated across 2015-16 incubations (Table S4) indicates that nitrification would be unlikely to fix more than 1 µmol L-1, in comparison to OC gains 601 ± 459 µM (mean $\pm$ 95% CI of SE <20 µm incubation, Fig, 3B, Table S4). Chemolithoautotrophy by sulfur oxidizing bacteria can also sequester carbon (Klatt and Polerecky, 2015), with the ratio of CO_2 sequestered to O_2 consumed ranging from 0.09 – 0.41 for aerobic

280 thiosulfate oxidizers (Klatt and Polerecky, 2015). Given the high sediment concentration in streams affected by slumping (can exceed 800 g L-1, Shakil et al. 2020), and the prevalence of sulfide minerals and oxidation across the Peel Plateau (Zolkos et al., 2018), chemolithoautotrophy associated with sulfide oxidation is a mechanism worth exploring as a counterbalance to OC mineralization. Precise techniques such as isotope labelling (Spona-Friedl et al., 2020) and the tracking of genes associated with carbon fixation processes (Percak-Dennett et al., 2017) may circumvent challenges associated with POC measurement

285 errors and tracking multiple processes acting on OC end-point measurements.

This study and Tanski et al. (2019) both suggest DOC contributes more to heterotrophic CO_2 production than POC in glacial margin landscapes. This seemingly contrasts protection of DOM by adsorption (Littlefair et al., 2017), however adsorption onto minerals tends to favour humic-like, oxygen-rich compounds, typically considered recalcitrant, over protein-like compounds (Groeneveld et al., 2020). Thus, sorption could "sort" labile carbon into the dissolved phase and relegate

290 intrinsically recalcitrant ("humic-like", aromatic) carbon to mineral protection as POC. Evidence of this includes elevated lability of slump-mobilized DOM relative to upstream DOM (Littlefair et al., 2017; Littlefair and Tank, 2018), low lability of slump POM (Shakil et al., 2020; this study) and striking compositional similarity of DOC from slump-impacted streams on the Peel Plateau relative to other circumpolar regions with mineral soils (e.g., Yedoma regions)(Wologo et al., 2021). Where RTS sediments continue to sequester aromatic DOM during fluvial transport, the relative increase in lability in the remaining

295 DOM pool may promote microbial OC oxidation and CO_2 production downstream. However, when particles settle out, anoxia could result in release of adsorbed DOC to the overlying water column (Peter et al., 2016), which may explain the switch from mean DOC decreases to DOC increase in comparisons between rotated and settled slump treatments in 2015. Sorption appeared to occur in 2019 sterilized bottles as DOC concentrations declined but POC increased, and DOM aromaticity and molecular weight decreased. No change in DOM in unsterilized bottles may reflect sorption (loss of aromaticity) and degradation (gain

300 of aromaticity) acting simultaneously, which underlines challenges in quantifying process by measuring OC changes in bulk incubations and why DOC declines were not consistently followed by increases or decreases in $SUVA_{254}$ across experiments, even when losses were consistent as in 2016.

5 Conclusion

305 Permafrost thaw slumping is increasing permafrost OC concentrations in streams across the Peel Plateau (Canada) by orders of magnitude, almost entirely in the form of POC (Kokelj et al., 2020; Shakil et al., 2020; Keskitalo et al., 2021). We find slump-POC has low biodegradability in streams, with >90% likely to be sequestered in sediments after mobilization to streams. Increased input of minerals into streams creates potential for significant abiotic (sorption, mineral protection) and biotic (chemolithotrophy) sequestration effects. Targeted investigations of these multiple processes acting simultaneously on carbon

310 dynamics require specific quantification in landscapes experiencing rapid change.

Appendices

Appendix A: Data analysis details and ANOVA results

The percent change of OC was used to measure differences in biodegradability:

$$\%\Delta OC = \frac{(OC_{T_n} - OC_{TOaverage})}{OC_{TOaverage}} \tag{A1}$$

315 In eq. 1 above, OC_{T_n} is the DOC, POC, or TOC measured at an end time point, and $OC_{TOaverage}$ is the mean OC measured at the beginning of the experiment. Since multiple outcomes were tested for ANOVAs, p-values of main tests were corrected for false discovery rate using padjust() from R package "emmeans" (Lenth, 2021). For 2015, main tests were corrected for 19 tests since SU treatments was tested in 4 comparisons and 3-4 outcomes were tested per comparison. For 2016, main tests were corrected for 4-5 tests since 4-5 outcomes were tested per ANOVA. Follow-up Tukey or Games-Howell adjusted pairwise t-

320 tests were conducted only when an interaction or main test of interest was significant. Prior to PCA we (a) used Pearson correlations to remove variables such that no variables within the PCA had a Pearson correlation greater than 0.9; (b) log-transformed all variables to prevent skew and (c) conducted a detrended correspondence analysis to ensure linearity of the dataset.

325 **Table A1: Two-way ANOVAs of tests of sources, filtrate, and settling on biodegradability of POC in 2015 experiments. Follow-up tukey-adjusted pair-wise t-tests are shown where significant interactions were present. Since SU treatments were tested 3 times and multiple outcomes were tested, p-values reported in two-way ANOVAs were corrected for false discovery rate (FDR) (19 tests). Degrees of freedom associated with treatment, site, interaction, and residuals are 1, 2, 2, and 12 respectively for all tests.**

Effect		Treatment				Site		Treatment*Site	
Test	Variable	estimate	error	F/t[a]	p	F	p	F	p
Control	$\Delta SUVA_{254}$	-	-	1.45	0.48	1.64	0.37	1.42	0.66
(SU-UF)	$\%\Delta DOC$	-	-	0.54	0.75	0.02	0.98	0.54	0.81
	$\%\Delta TOC$	-	-	0.49	0.75	0.07	0.98	0.98	0.80
	$\ln(k)$	-	-	305.57	**0.00**	6.43	**0.04**	8.92	**0.04**

	HA	2.01	0.17	11.80	<<.001	-	-	-	-
	HB	2.02	0.17	11.83	<<.001	-	-	-	-
	HD	1.13	0.17	6.64	<<.001	-	-	-	-
Source	ΔSUVA$_{254}$			2.22	0.34	0.14	0.98	6.51	0.08
(SU-UU)	*HA*	*0.40*	*0.11*	*3.80*	0.00	-	-	-	-
	HB	*-0.06*	*0.11*	*-0.52*	0.61	-	-	-	-
	HD	*-0.07*	*0.11*	*-0.70*	0.50	-	-	-	-
	%ΔDOC	-7.06	2.46	8.22	0.05	1.13	0.47	1.53	0.66
	log(%POC+50)	-0.19	0.04	27.40	0.00	5.08	0.07	2.39	0.42
	%ΔTOC	-	-	2.22	0.34	1.73	0.37	0.78	0.80
	ln(k)			172.43	0.00	43.21	0.00	67.84	0.00
	HA	*1.69*	*0.15*	*11.60*	**<<.001**	-		-	
	HB	*1.90*	*0.15*	*13.04*	**<<.001**	-		-	
	HD	*-0.28*	*0.15*	*-1.89*	**0.08**	-		-	
Filtrate	ΔSUVA$_{254}$	-	-	2.52	0.34	11.81	**0.01**	0.41	0.81
(SD-SU)	%ΔDOC	-	-	0.05	0.87	2.71	0.21	2.90	0.42
	%ΔPOC	-	-	0.11	0.85	2.66	0.21	0.20	0.89
	%ΔTOC	-	-	0.37	0.75	2.66	0.21	0.72	0.80
	k	-	-	0.24	0.81	20.12	**0.00**	0.19	0.88
Settling	ΔSUVA$_{254}$	-	-	0.10	0.85	10.46	**0.01**	0.77	0.80
(SS-SU)	%ΔDOC	-	-	5.84	0.10	0.11	0.98	0.39	0.81
	%ΔPOC	-	-	0.38	0.75	1.08	0.47	0.21	0.88
	%ΔTOC	-	-	0.00	0.96	1.36	0.43	0.43	0.81
	ln(k)	-0.67	0.07	81.68	**0.00**	11.47	**0.01**	2.46	0.42

330 [a]F-values are reported for two-way ANOVAS, t-values are reported for follow-up pairwise t-tests

Table A2: Welch's ANOVA and follow-up games-howell pair-wise t-tests of differences between size fractions (2016 experiment). P-values for main ANOVAs are adjusted for false-discovery rate (fdr) to account for multiples outcomes tested (5 tests). Follow-up tests were only conducted when main ANOVA tests showed a significant difference. Size
335 **fractions: SN = 63 – 2000 μm, SL= 20 – 63 μm, SMSC = <20 μm.**

Variable	F	df$_{num}$	df$_{denom}$	p	Follow-up tests				
					Estimate	95% error	t	df	p
ΔSUVA$_{254}$[a]	41.63	2	5.8	**0.001**					
	SL vs SN				2.00E-02	1.75E-01	0.46	5.2	0.894
	SMSC vs SN				3.80E-01	1.75E-01	7.14	5.0	**0.002**
	SMSC vs SL				3.60E-01	2.60E-01	8.62	6.0	**<0.001**
%ΔDOC	22.21	2	4.9	**0.007**					

SL vs SN				-6.09E+00	1.97E+01	2.00	4.8	0.200	
SMSC vs SN				-1.45E+01	2.00E+01	5.40	3.4	**0.018**	
SMSC vs SL				-8.39E+00	1.12E+01	5.20	4.3	**0.012**	
%ΔPOC	2.81	2	4.5	0.161					
%ΔTOC	5.13	2	4.4	0.089					
ln(k)	66.66	2	5.9	**<0.001**					
SL vs SN				-4.34E-05	4.01E-03	-0.01	9.0	0.992	
SMSC vs SN				3.87E-02	4.01E-03	9.66	9.0	**<<0.001**	
SMSC vs SL				3.87E-02	4.01E-03	9.67	9.0	**<<0.001**	

Table A3: Two-way ANOVAs for transect experiment examining effects of filtrations (unfiltered vs. filtered) and distance (immediately downstream vs. 2.79 km downstream) from slump SE and interactions between the two. Since multiple (4-5) parameters from the same experiment are tested, p-values were corrected for false discovery rate (FDR). Degrees of freedom associated with distance, filtration, interaction, and residuals are 1, 1, 1, and 12 respectively for all tests.

Variable	Distance		Filtration		Distance*Filtration		Follow-up tests				
	F	p	F	p	F	p	Est.	se	t	df	p
ΔSUVA254	0.21	0.659	5.59	0.048	12.44	0.013					
DN vs 2.79 km DN (filtered)							-0.09	0.04	-2.174	12	0.050
DN vs 2.79 km DN (unfiltered)							0.12	0.04	2.815	12	0.016
%ΔDOC	7.39	0.031	17.00	0.003	10.87	0.013					
DN vs 2.79 km DN (filtered)							0.67	1.64	0.409	12	0.689
DN vs 2.79 km DN (unfiltered)							-6.96	1.64	-4.253	12	0.001
%ΔPOC[a]	12.01	0.031	-	-	-	-					
%ΔTOC	1.71	0.269	1.99	0.184	0.00	0.949					
ln(k)	12.65	0.020	55.96	0.000	0.95	0.466					

[a]Percent change in POC not tested for filtration or interaction effect because negligible POC concentrations in filtered treatments

345 **Appendix B: Characterization of each size fraction**

Size fractions with lower particles sizes had lower organic matter content (lower percent organic carbon) and associated organic matter had a greater 14C age (Table B1). Extraction of size fractions was done in triplicate, but one replicate of the size fraction > 63 µm had to be removed due to optical density concerns (supplementary S3.8). A biplot of PCA components 1 and 2 that explained 92% of the variation in optical indices of BEPOM revealed that extractions of organic matter in the clay and silt size

350 fractions had a greater relative contribution of UVA humic-like peak C (Fig. B1), which has been characterized as terrigenous organic matter that has undergone less chemical reworking than peak A (Stubbins et al. 2014). While peak C was not negatively correlated with peak A, it was strongly correlated with total absorbance per unit of sediment extracted (Table S6).

Table B1: Characteristics of size fractions used in 2016 experiment. %POC indicates POC: TSS. sd = standard
355 **deviation. SEM = standard error of the mean.**

Size Fraction Category	Unfractionated	0.063 - 2mm	0.020 - 0.063 mm	<0.020 mm
Mean particle size	11.9	48.9	21.67	5.78
sd	3.78	4.6	2.9	2.79
$F^{14}C$	NA	0.4113	0.1332	0.056
sd	NA	0.0019	0.0012	0.0006
calBP (percent representation)	NA	8020 - 7926 (88.3%)	19791 - 19292 (95.4%)	27640 - 27250 (95.4%)
		7896 - 7871 (7.1%)		
%POC	1.6	3.12	1.35	1.67
SEM	0.03	0.09	0.02	0.02
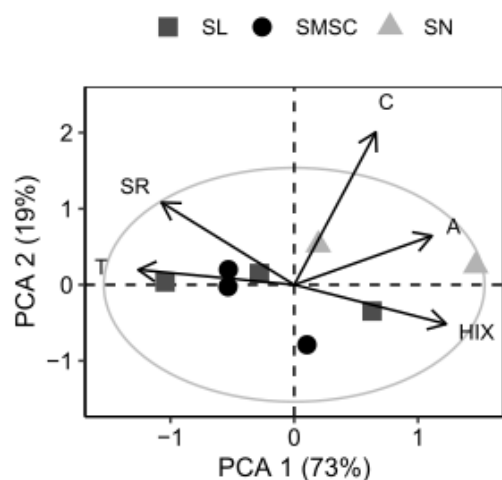
Figure A1: Principal components analysis of optical indices for BEPOM of different size fractions. PCA is shown in scaling 1. The grey circle marks the circle of equilibrium contribution. Constituent abbreviations are as in Table S5.

Appendix C: Absolute changes in SUVA$_{254}$

Table C1: Absolute changes in SUVA$_{254}$ in 2015-16 experiments.

Year	Treatment	Site	ΔSUVA$_{254}$	95% error	n
2015	Filtered upstream (F)	HA	0.08	0.36	3
		HB	0.11	0.70	3
		HD	0.02	0.08	3
	Unfiltered upstream (U)	HA	-0.25	0.20	3
		HB	-0.06	0.35	3
		HD	-0.02	0.44	3
	Slump in filtered upstream (SU)	HA	0.16	0.47	3
		HB	-0.11	0.16	3
		HD	-0.09	0.15	3
	Slump in filtered downstream (SD)	HA	0.20	0.28	3
		HB	-0.07	0.06	3
		HD	0.04	0.12	3
	SU settle (SS)	HA	0.19	0.41	3
		HB	-0.05	0.20	3
		HD	-0.20	0.60	2
2016	Unfractionated	SE	0.46	0.41	4
	2 - 0.063 mm	SE	0.06	0.15	4
	0.063 - 0.020 mm	SE	0.09	0.10	4
	< 0.020 mm	SE	0.45	0.09	4
	Upstream	SE	-0.07	0.11	4
	Upstream filtered control	SE	-0.07	0.07	4
	Downstream	SE	-0.10	0.17	4
	Downstream filtered control	SE	0.07	0.05	4
	2.79k Downstream	S2	-0.01	0.03	4
	2.79k Downstream filtered control	S2	-0.05	0.07	4

Code Availability

Code for this manuscript is available upon request.

Data Availability

Data will be made openly available through the Polar Data Catalogue (CCIN reference #: 13237). (Shakil et al. 2021)

365 **Supplement link**

A supplementary pdf file has been uploaded for review with this manuscript.

Author contribution

SS and SET led the design of the study. SS led data collection, data analysis and interpretation, and manuscript writing. JEV contributed to the initial development of the idea, and JEV and SZ contributed to study design and data interpretation. SZ
370 contributed to laboratory methods for data collection. All authors contributed to manuscript writing.

Competing interests

The authors declare they have no conflict of interest.

Acknowledgements

This work took place within the Gwich'in Settlement Region, and we are thankful for support from the Tetlit Gwich'in
375 Renewable Resources Council and Western Arctic Research Centre. We are further thankful for the field assistance of Christine Firth, Elizabeth Jerome, Andrew Koe, Joyce Kendon, Maya Guttman, Luke Gjini, and Lindsay Stephen. Maya Guttman and Joyce Kendon also helped experiment set up and sample processing. Hailey Verbonac assisted with O_2 measurements during our 2015 experiments conducted in Inuvik. This manuscript also benefitted from helpful discussions with: Steve Kokelj with regards to field sampling and perspectives on landscape changes in the region; and Matthias Koschorreck and Rafael Marcé
380 with regards to chemoautotrophic processes, and Alex Wolfe who first provided advice to broaden consideration of what affects oxygen and carbon dynamics. Funding for this study was provided by the Natural Sciences and Engineering Research Council (NSERC), Polar Continental Shelf Program (Natural Resources Canada), Campus Alberta Innovates Program, ArcticNet, CiCan Cleantech Internship Program, Environment Canada Science Youth Horizons Internship, Northern Scientific Training Program, University of Alberta and UAlberta North, and the Aurora Research Institute. Personal support to SS was
385 provided by NSERC and the Garfield Weston Foundation. Research for this paper was conducted under NWT research licences: 15685 (2015); 15685 (2016); 15887 (2017); 16575 (2019).

References

Abbott, B. W., Larouche, J. R., Jones, J. B., Bowden, W. B., and Balser, A. W.: Elevated dissolved organic carbon biodegradability from thawing and collapsing permafrost, J. Geophys. Res. Biogeosciences, 119, 2049–2063,
390 https://doi.org/10.1002/2014JG002678, 2014.

Attermeyer, K., Catalán, N., Einarsdottir, K., Freixa, A., Groeneveld, M., Hawkes, J. A., Bergquist, J., and Tranvik, L. J.: Organic Carbon Processing During Transport Through Boreal Inland Waters: Particles as Important Sites, J. Geophys. Res. Biogeosciences, 123, 2412–2428, https://doi.org/10.1029/2018JG004500, 2018.

395 Berggren, M., Lapierre, J.-F., and del Giorgio, P. A.: Magnitude and regulation of bacterioplankton respiratory quotient across freshwater environmental gradients, ISME J., 6, 984–993, https://doi.org/10.1038/ismej.2011.157, 2012.

Bock, E. and Wagner, M.: Oxidation of Inorganic Nitrogen Compounds as an Energy Source, in: The Prokaryotes, edited by: Rosenberg, E., DeLong, E. F., Lory, S., Stackebrandt, E., and Thompson, F., Springer Berlin Heidelberg, Berlin, Heidelberg, 83–118, https://doi.org/10.1007/978-3-642-30141-4_64, 2013.

400 Bröder, L., Keskitalo, K., Zolkos, S., Shakil, S., Tank, S. E., Kokelj, S. V., Tesi, T., van Dongen, B. E., Haghipour, N., Eglinton, T. I., and Vonk, J. E.: Preferential export of permafrost-derived organic matter as retrogressive thaw slumping intensifies, Environ. Res. Lett., https://doi.org/10.1088/1748-9326/abee4b, 2021.

Coble, P. G.: Marine Optical Biogeochemistry: The Chemistry of Ocean Color, Chem. Rev., 107, 402–418, https://doi.org/10.1021/cr050350%2B, 2007.

405 Duk-Rodkin, A., and Hughes, O. L.: Surficial geology, Fort McPherson-Bell River, Yukon-Northwest Territories. Geological Survey of Canada, 1992.

Groeneveld, M., Catalán, N., Attermeyer, K., Hawkes, J., Einarsdóttir, K., Kothawala, D., Bergquist, J., and Tranvik, L.: Selective Adsorption of Terrestrial Dissolved Organic Matter to Inorganic Surfaces Along a Boreal Inland Water Continuum, J. Geophys. Res. Biogeosciences, 125, e2019JG005236, https://doi.org/10.1029/2019JG005236, 2020.

410 Hemingway, J. D., Rothman, D. H., Grant, K. E., Rosengard, S. Z., Eglinton, T. I., Derry, L. A., and Galy, V. V.: Mineral protection regulates long-term global preservation of natural organic carbon, Nature, 570, 228–231, https://doi.org/10.1038/s41586-019-1280-6, 2019.

Hugelius, G., Strauss, J., Zubrzycki, S., Harden, J. W., Schuur, E. A. G., Ping, C.-L., Schirrmeister, L., Grosse, G., Michaelson, G. J., Koven, C. D., O'Donnell, J. A., Elberling, B., Mishra, U., Camill, P., Yu, Z., Palmtag, J., and Kuhry, P.: Estimated stocks of circumpolar permafrost carbon with quantified uncertainty ranges and identified data gaps, 415 Biogeosciences, 11, 6573–6593, https://doi.org/10.5194/bg-11-6573-2014, 2014.

Keskitalo, K. H., Bröder, L., Shakil, S., Zolkos, S., Tank, S. E., van Dongen, B. E., Tesi, T., Haghipour, N., Eglinton, T. I., Kokelj, S. V., and Vonk, J. E.: Downstream Evolution of Particulate Organic Matter Composition From Permafrost Thaw Slumps, Front. Earth Sci., 9, https://doi.org/10.3389/feart.2021.642675, 2021.

Klatt, J. M. and Polerecky, L.: Assessment of the stoichiometry and efficiency of CO2 fixation coupled to reduced sulfur 420 oxidation, Front. Microbiol., 6, https://doi.org/10.3389/fmicb.2015.00484, 2015.

Kokelj, S. V., Kokoszka, J., van der Sluijs, J., Rudy, A. C. A., Tunnicliffe, J., Shakil, S., Tank, S., and Zolkos, S.: Permafrost thaw couples slopes with downstream systems and effects propagate through Arctic drainage networks, Cryosphere Discuss., 1–43, https://doi.org/10.5194/tc-2020-218, 2020.

Kothawala, D. N., Kellerman, A. M., Catalán, N., and Tranvik, L. J.: Organic Matter Degradation across Ecosystem 425 Boundaries: The Need for a Unified Conceptualization, Trends Ecol. Evol., 36, 113–122, https://doi.org/10.1016/j.tree.2020.10.006, 2021.

Lacelle, D., Fontaine, M., Pellerin, A., Kokelj, S. V., and Clark, I. D.: Legacy of Holocene Landscape Changes on Soil Biogeochemistry: A Perspective From Paleo-Active Layers in Northwestern Canada, J. Geophys. Res. Biogeosciences, 124, 2662–2679, https://doi.org/10.1029/2018JG004916, 2019.

430 Lenth, R. V.: emmeans: Estimated Marginal Means, aka Least-Squares Means. R package version 1.6.0. https://CRAN.R-project.org/package=emmeans, 2021.

Littlefair, C. A. and Tank, S. E.: Biodegradability of Thermokarst Carbon in a Till-Associated, Glacial Margin Landscape: The Case of the Peel Plateau, NWT, Canada, J. Geophys. Res. Biogeosciences, 123, 3293–3307, https://doi.org/10.1029/2018JG004461, 2018.

435 Littlefair, C. A., Tank, S. E., and Kokelj, S. V.: Retrogressive thaw slumps temper dissolved organic carbon delivery to streams of the Peel Plateau, NWT, Canada, Biogeosciences, 14, 5487–5505, https://doi.org/10.5194/bg-14-5487-2017, 2017.

Mann, P. J., Eglinton, T. I., McIntyre, C. P., Zimov, N., Davydova, A., Vonk, J. E., Holmes, R. M., and Spencer, R. G. M.: Utilization of ancient permafrost carbon in headwaters of Arctic fluvial networks, Nat. Commun., 6, 7856, https://doi.org/10.1038/ncomms8856, 2015.

440 Nelson, D. C., Jørgensen, B. B., and Revsbech, N. P.: Growth Pattern and Yield of a Chemoautotrophic Beggiatoa sp. in Oxygen-Sulfide Microgradients, Appl. Environ. Microbiol., 52, 225–233, 1986.

Olefeldt, D., Goswami, S., Grosse, G., Hayes, D., Hugelius, G., Kuhry, P., McGuire, A. D., Romanovsky, V. E., Sannel, A. B. K., Schuur, E. A. G., and Turetsky, M. R.: Circumpolar distribution and carbon storage of thermokarst landscapes, Nat. Commun., 7, 13043, https://doi.org/10.1038/ncomms13043, 2016.

445 Opfergelt, S.: The next generation of climate model should account for the evolution of mineral-organic interactions with permafrost thaw, Environ. Res. Lett., 15, 091003, https://doi.org/10.1088/1748-9326/ab9a6d, 2020.

Osburn, C. L., Handsel, L. T., Mikan, M. P., Paerl, H. W., and Montgomery, M. T.: Fluorescence Tracking of Dissolved and Particulate Organic Matter Quality in a River-Dominated Estuary, Environ. Sci. Technol., 46, 8628–8636, https://doi.org/10.1021/es3007723, 2012.

450 Percak-Dennett, E., He, S., Converse, B., Konishi, H., Xu, H., Corcoran, A., Noguera, D., Chan, C., Bhattacharyya, A., Borch, T., Boyd, E., and Roden, E. E.: Microbial acceleration of aerobic pyrite oxidation at circumneutral pH, Geobiology, 15, 690–703, https://doi.org/10.1111/gbi.12241, 2017.

Peter, S., Isidorova, A., and Sobek, S.: Enhanced carbon loss from anoxic lake sediment through diffusion of dissolved organic carbon, J. Geophys. Res. Biogeosciences, 121, 1959–1977, https://doi.org/10.1002/2016JG003425, 2016.

455 Richardson, D. C., Newbold, J. D., Aufdenkampe, A. K., Taylor, P. G., and Kaplan, L. A.: Measuring heterotrophic respiration rates of suspended particulate organic carbon from stream ecosystems: Measuring respiration rates of POC, Limnol. Oceanogr. Methods, 11, 247–261, https://doi.org/10.4319/lom.2013.11.247, 2013.

Schuur, E. A. G., McGuire, A. D., Schädel, C., Grosse, G., Harden, J. W., Hayes, D. J., Hugelius, G., Koven, C. D., Kuhry, P., Lawrence, D. M., Natali, S. M., Olefeldt, D., Romanovsky, V. E., Schaefer, K., Turetsky, M. R., Treat, C. C., and Vonk, J.
460 E.: Climate change and the permafrost carbon feedback, Nature, 520, 171–179, https://doi.org/10.1038/nature14338, 2015.

Segal, R. A., Lantz, T. C., and Kokelj, S. V.: Acceleration of thaw slump activity in glaciated landscapes of the Western Canadian Arctic, Environ. Res. Lett., 11, 034025, https://doi.org/10.1088/1748-9326/11/3/034025, 2016.

Shakil, S., Tank, S. E., Kokelj, S. V., Vonk, J. E., and Zolkos, S.: Particulate dominance of organic carbon mobilization from thaw slumps on the Peel Plateau, NT: Quantification and implications for stream systems and permafrost carbon release, Environ. Res. Lett., 15, 114019, https://doi.org/10.1088/1748-9326/abac36, 2020.

Shakil, S., Tank, S., Vonk J.E., and Zolkos S.: Incubation Data Assessing Biodegradability of Organic Carbon Mobilized from Permafrost Thaw Slumps (Peel Plateau, NT, Canada). Waterloo, Canada: Canadian Cryospheric Information Network (CCIN). (DOI TBD), 2021.

Sinha, B. and Annachhatre, A. P.: Partial nitrification—operational parameters and microorganisms involved, Rev. Environ. Sci. Biotechnol., 6, 285–313, https://doi.org/10.1007/s11157-006-9116-x, 2007.

Spona-Friedl, M., Braun, A., Huber, C., Eisenreich, W., Griebler, C., Kappler, A., and Elsner, M.: Substrate-dependent CO2 fixation in heterotrophic bacteria revealed by stable isotope labelling, FEMS Microbiol. Ecol., 96, fiaa080, https://doi.org/10.1093/femsec/fiaa080, 2020.

Stolper, D. A., Revsbech, N. P., and Canfield, D. E.: Aerobic growth at nanomolar oxygen concentrations, Proc. Natl. Acad. Sci., 107, 18755–18760, https://doi.org/10.1073/pnas.1013435107, 2010.

Tank, S. E., Vonk, J. E., Walvoord, M. A., McClelland, J. W., Laurion, I., and Abbott, B. W.: Landscape matters: Predicting the biogeochemical effects of permafrost thaw on aquatic networks with a state factor approach, Permafr. Periglac. Process., 31, 358–370, https://doi.org/10.1002/ppp.2057, 2020.

Tanski, G., Lantuit, H., Ruttor, S., Knoblauch, C., Radosavljevic, B., Strauss, J., Wolter, J., Irrgang, A. M., Ramage, J., and Fritz, M.: Transformation of terrestrial organic matter along thermokarst-affected permafrost coasts in the Arctic, Sci. Total Environ., 581–582, 434–447, https://doi.org/10.1016/j.scitotenv.2016.12.152, 2017.

Tanski, G., Wagner, D., Knoblauch, C., Fritz, M., Sachs, T., and Lantuit, H.: Rapid CO2 Release From Eroding Permafrost in Seawater, Geophys. Res. Lett., 46, 11244–11252, https://doi.org/10.1029/2019GL084303, 2019.

Tesi, T., Semiletov, I., Dudarev, O., Andersson, A., and Gustafsson, Ö.: Matrix association effects on hydrodynamic sorting and degradation of terrestrial organic matter during cross-shelf transport in the Laptev and East Siberian shelf seas, J. Geophys. Res. Biogeosciences, 121, 731–752, https://doi.org/10.1002/2015JG003067, 2016.

Turetsky, M. R., Abbott, B. W., Jones, M. C., Anthony, K. W., Olefeldt, D., Schuur, E. A. G., Grosse, G., Kuhry, P., Hugelius, G., Koven, C., Lawrence, D. M., Gibson, C., Sannel, A. B. K., and McGuire, A. D.: Carbon release through abrupt permafrost thaw, Nat. Geosci., 13, 138–143, https://doi.org/10.1038/s41561-019-0526-0, 2020.

Vachon, D., Sadro, S., Bogard, M. J., Lapierre, J.-F., Baulch, H. M., Rusak, J. A., Denfeld, B. A., Laas, A., Klaus, M., Karlsson, J., Weyhenmeyer, G. A., and Giorgio, P. A. del: Paired O2–CO2 measurements provide emergent insights into aquatic ecosystem function, Limnol. Oceanogr. Lett., 5, 287–294, https://doi.org/10.1002/lol2.10135, 2020.

Vonk, J. E., Tank, S. E., Mann, P. J., Spencer, R. G. M., Treat, C. C., Striegl, R. G., Abbott, B. W., and Wickland, K. P.: Biodegradability of dissolved organic carbon in permafrost soils and aquatic systems: a meta-analysis, Biogeosciences, 12, 6915–6930, https://doi.org/10.5194/bg-12-6915-2015, 2015a.

Vonk, J. E., Tank, S. E., Bowden, W. B., Laurion, I., Vincent, W. F., Alekseychik, P., Amyot, M., Billet, M. F., Canário, J., Cory, R. M., Deshpande, B. N., Helbig, M., Jammet, M., Karlsson, J., Larouche, J., MacMillan, G., Rautio, M., Walter Anthony, K. M., and Wickland, K. P.: Reviews and syntheses: Effects of permafrost thaw on Arctic aquatic ecosystems, Biogeosciences, 12, 7129–7167, https://doi.org/10.5194/bg-12-7129-2015, 2015b.

500 Weishaar, J. L., Aiken, G. R., Bergamaschi, B. A., Fram, M. S., Fujii, R., and Mopper, K.: Evaluation of Specific Ultraviolet Absorbance as an Indicator of the Chemical Composition and Reactivity of Dissolved Organic Carbon, Environ. Sci. Technol., 37, 4702–4708, https://doi.org/10.1021/es030360x, 2003.

Wologo, E., Shakil, S., Zolkos, S., Textor, S., Ewing, S., Klassen, J., Spencer, R. G. M., Podgorski, D. C., Tank, S. E., Baker, M. A., O'Donnell, J. A., Wickland, K. P., Foks, S. S. W., Zarnetske, J. P., Lee-Cullin, J., Liu, F., Yang, Y., Kortelainen, P.,
505 Kolehmainen, J., Dean, J. F., Vonk, J. E., Holmes, R. M., Pinay, G., Powell, M. M., Howe, J., Frei, R. J., Bratsman, S. P., and Abbott, B. W.: Stream Dissolved Organic Matter in Permafrost Regions Shows Surprising Compositional Similarities but Negative Priming and Nutrient Effects, Glob. Biogeochem. Cycles, 35, e2020GB006719, https://doi.org/10.1029/2020GB006719, 2021.

Zar, J. H.: Biostatistical Analysis, 5th ed., Prentice Hall, Upper Saddle River, N.J., 944 pp., 2010.

510 Zolkos, S. and Tank, S. E.: Experimental Evidence That Permafrost Thaw History and Mineral Composition Shape Abiotic Carbon Cycling in Thermokarst-Affected Stream Networks, Front. Earth Sci., 8, https://doi.org/10.3389/feart.2020.00152, 2020.

Zolkos, S., Tank, S. E., and Kokelj, S. V.: Mineral Weathering and the Permafrost Carbon-Climate Feedback, Geophys. Res. Lett., 45, 9623–9632, https://doi.org/10.1029/2018GL078748, 2018.

515 Zolkos, S., Tank, S. E., Striegl, R. G., and Kokelj, S. V.: Thermokarst Effects on Carbon Dioxide and Methane Fluxes in Streams on the Peel Plateau (NWT, Canada), J. Geophys. Res. Biogeosciences, 124, 1781–1798, https://doi.org/10.1029/2019JG005038, 2019.

Zolkos, S., Tank, S. E., Striegl, R. G., Kokelj, S. V., Kokoszka, J., Estop-Aragonés, C., and Olefeldt, D.: Thermokarst amplifies fluvial inorganic carbon cycling and export across watershed scales on the Peel Plateau, Canada, Biogeosciences, 17, 5163–
520 5182, https://doi.org/10.5194/bg-17-5163-2020, 2020.